Turkish Journal of Agriculture - Food Science and Technology, 13(2): 453-463, 2025
DOI: https://doi.org/10.24925/turjaf.v13i2.453-463.7382

Turkish Journal of Agriculture - Food Science and Technology

Available online, ISSN: 2148-127X | www.agrifoodscience.com | Turkish Science and Technology Publishing (TURSTEP)

Synthesis of Modified Poly (glycidyl methacrylate) (PGMA) Hydrogels, and Investigation of Their Potential in Dye Removal

Kübra Gülcemal[1,a], Kutalmış Gökkuş[1,b,*]

[1]*Kastamonu University, Faculty of Engineering, and Architecture Department of Environmental Engineering, 37500, Kastamonu, Türkiye*
[*]*Corresponding author*

ARTICLE INFO

Research Article

Received : 04.12.2024
Accepted : 21.12.2024

Keywords:
Poly (glycidyl methacrylate)
Isotherm
Adsorption
Bromophenol blue
Anthropogenic activities

ABSTRACT

Anthropogenic activities with increasing population lead the pollution of ecosystems. Over one-third of the world's water resources are utilized for agricultural, domestic, and industrial activities, resulting in contamination by synthetic, and geogenic compounds such as dyes, fertilizers, pesticides, and heavy metals. Among these pollutants, dyes are particularly noteworthy due to their extensive use across various sectors, making them one of the leading contributors to water pollution. For this reason, dyes are one of the most important pollutants that cause water pollution. Therefore, the adsorption of Bromophenol blue (BPB) was studied in this study. Firstly, PGMA gels were produced by polymerizing of glycidyl methacrylate (GMA) monomer. Secondly, the PGMA gels were modified to prepare the new adsorbents for the adsorption of BPB dye. Thirdly, the adsorption of BPB dye was carried out. The batch adsorption method was used. The optimum adsorbent amount, initial BPB concentration, pH, and temperature parameters for PGMA gels were determined. The adsorption mechanism between modified PGMA gels, and BPB dye was elucidated by Langmuir, Freundlich, Dubinin-Radushkevich, and Temkin isotherm models. As a result, it was seen that modified PGMA gels showed good performance in the adsorption of BPB.

[a] *kubraglcmlkgl@gmail.com* *https://orcid.org/0009-0005-2533-2305* | [b] *kgokkus@kastamonu.edu.tr* *https://orcid.org/0000-0002-4016-4283*

Introduction

Organic dyes are one of the most commonly used and therefore most common hazardous organic pollutants in the environment. The main sources of dyes are primarily leather, textile, plastic, paper, cosmetic, and food industries (Namasivayam et al., 1994). The wastewaters discahrged as a result of dyeing processes contain generally high levels of colored components, and this not only causes aesthetic discomfort but also negatively affects biological processes in water bodies. It is well known that azo dyes (e.g. aromatic amines and azo groups) are carcinogenic (Malik, 2004).

The estimates reveal that each year, approximately 12% of synthetic textile dyes are directly discharged during production processes without treatment (Morais et al., 1999). Dyes such as bromophenol blue are frequently preferred compounds for coloring purposes. However, the discharge of these dyes into water resources without treatment poses significant environmental threats by creating toxic effects on both human health, and natural life (Yao et al., 2020). For example, dyes can cause allergic reactions and skin irritation in humans; many of them are also mutagenic and/or carcinogenic (Ghaedi et al., 2013). In addition, dyes cause water to become colored even in very low concentrations (<1 mg/L). This reduces the transparency of the water, negatively affecting photosynthesis and leading to a decrease in the level of dissolved oxygen (Moradihamedani, 2022).

The removal of dyes from wastewaters is still continued a significant environmental problem and technical challenge. In an effective dye treatment method, large amounts of dyes should be rapidly removed while not causing secondary pollution (Katheresan et al., 2018). To date, various chemical, biological, and physical methods were developed for the dye removal (Mashkoor & Nasar, 2020). Although there are many methods in the literature, most of them are not used due to their lack of sustainability and high costs. For example, biological methods can be effective in removing industrial dyes via biodegradation. However, for biological methods, relatively large areas are required. In addition, these methods are easily affected by environmental conditions. Therefore, the use of these methods is limited. In chemical methods, such as coagulation, ion exchange resins, and advanced oxidation are used; however, these methods are generally high-cost,

and can lead to the formation of undesirable by-products. In other hand, although physical methods such as filtration, and adsorption also have some limitations (Raman & Kanmani, 2016, Mezohegyi et al., 2012), the adsorption method is the most common method for the removal of dyes from industrial wastewater due to its high efficiency, ease of use and low cost. Adsorption stands out as an attractive alternative because it can effectively remove various types of dyes without by-products in wastewater (Mokif, 2019).

In light of the above information, this study aimed to efficiently remove BPB dye, which is widely used in the industry via adsorption method (El-Zahhar et al., 2014; Akpomie et al., 2024). In this context, PGMA gels were synthesized. Then, these gels were modified and characterized. Lastly, the performance of these gels in the adsorption of BPB dye was examined in detail.

Materials and Methods

Materials

N,N'-Methylenebisacrylamide (MBA, 99%), Glycidyl methacrylate (GMA, 97%), N,N,N',N'-Tetramethylethylenediamine (TEMED, 99%), and Ethylenediamine (EDA) were purchased from Merck, Ammonium peroxodisulphate (APS) from Sigma Aldrich, and Bromophenol blue (BPB, Mn: 669.96 g mol-1) was purchased from AFG Bioscience.

Synthesis of PGMA gels

PGMA gels were prepared using MBA as a crosslinker. For this, 65 mg (0.75% mol of PGMA) of MBA, and 6 mL of distilled water (DW) were added to 8.0 g of GMA. The mixture was stirred at room temperature for one hour using a magnetic stirrer. Subsequently, 400 µL of TEMED was added to the solution and vortexed for 1 minute, followed by the addition of 1 mol% (140 mg) of APS. The mixture was vortexed again for 2 minutes. Once the milky solution obtained, it was transferred into pipettes. These pipettes were placed on a tube shaker set at 70 rpm and left to react at room temperature for 24 hours. After the reaction was complete, the pipettes were carefully opened and the gels obtained. Then gels washed with DW for two days, and dried at 70°C. Finally, the dried gels were ground for subsequent characterization, and modification.

Modification of PGMA gels

PGMA gels were modified according to Gokkus et al. (2023). 4 g of PGMA gel, 16.9 g (0.28 mol, 10-fold of PGMA mole) EDA and 25 mL toluene were introduced to the round-bottomed reaction flask. The reaction was conducted 24 h at room temperature and then continued to the reaction at 80 °C for another 8 h. During this period, the solution was continuously stirred at low speed on a magnetic stirrer. End of the reaction, the modified PGMA gels were washed with ethanol, ethanol/distilled water (DW) mixture, and DW, respectively. Thus, PGMA-EDA gels were obtained (Figure 2).

The chemical structures of PGMA-EDA gels were revealed by FT-IR (Bruker, Alpha II), the structures, and gels' surface morphology were investigated by SEM (FEI Quanta FEG250), and their thermal stabilities were analysized by TGA-DTA analysis (Hitachi STA7300).

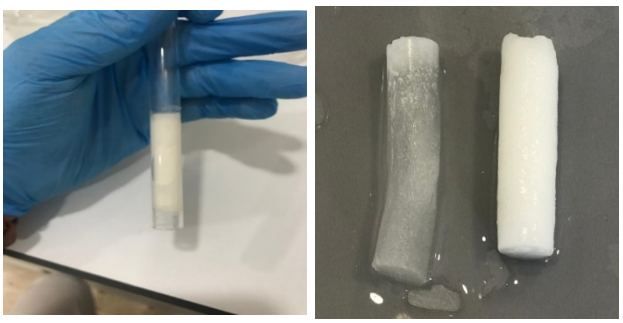

Figure 1. PGMA gels.

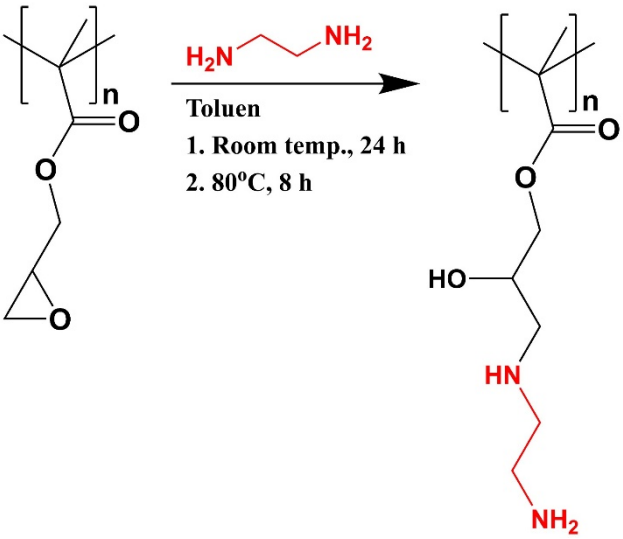

Figure 2. Modification of PGMA gels

Adsorption Experiments

Adsorption experiments were carried out in three replicates with batch adsorption method. In these studies, the effects of variables such as temperature (15 - 50 ºC), pH (2 - 10), contact time (60 - 360 min), initial dye concentration (20 - 500 ppm), and PGMA-EDA amount (5 - 50 mg) on PGMA-EDA gels' adsorption capacity were investigated. The solution volume was 10 mL, and the shaking speed was kept constant at 300 rpm in all adsorption experiments. The absorbance of BPB solutions was measured at 664 nm wavelength with Hach Lange DR9000 UV-VIS spectrophotometer. The adsorption capacity and efficiency (%) of removal calculations of PGMA-EDA gels were carried out using Equation (1), and Equation (2), respectively.

$$q_e = \frac{(C_o - C_e)}{W} V \quad (1)$$

$$\text{Dye removal (\%)} = \frac{(C_o - C_e)}{C_o} * 100\ \% \quad (2)$$

The solution volume is V (L), the initial, and final solution concentrations of BPB dye are Co, and Ce (mg L^{-1} or ppm), respectively and the adsorbed dry mass is W (g).

Adsorption Kinetics

The adsorption kinetics were examined to determine the equilibrium time of the adsorbent and the mechanism of BPB removal from wastewater. The resulting data were analyzed using pseudo-first-order (PFO; Lagergren, 1898), pseudo-second-order (PSO; Ho & McKay, 1999), Weber-Morris

intraparticle diffusion (ID; Weber & Morris, 1963), and Elovich (Benjelloun et al., 2021) kinetic models. The equations for the kinetic models are given below. (Eqs 3-6):

Pseudo-first order: $\ln(q_e - q_t) = \ln q_e - k_1.t$ (3)

Pseudo-second order: $t/q_t = 1/k_2.q_e^2 + t/q_e$ (4)

Intra particle diffusion: $q_t = k_{id}.\ t^{1/2} + I$ (5)

Elovich: $q_t=\beta \ln(\alpha\beta)-\ln(t)$ (6)

Where the dye amounts adsorbed, and at time t are q_e, and q_t, respectively. The equilibrium rate constants of PFO (1/min), PSO (g/mg.min), and ID model (mg/g.min$^{1/2}$) are k_1, k_2, and k_{id}, respectively.

Adsorption Isotherms

Experimental data were analyzed using Langmuir (Langmuir, 1916), Freundlich (Freundlich, 1906), Dubinin-Radushkevich (Radushkevich, 1947), and Temkin (Tempkin & Pyzhev 1940) isotherm models to assess the adsorption equilibrium. A detailed explanation of each isotherm model is provided below (Eq 7-13):

Langmuir

$$C_e/q_e = \frac{1}{q_{max}b} + \frac{1}{q_{max}}C_e \quad (7)$$

$$R_L = \frac{1}{1+bC_0} \quad (8)$$

Freundlich

$$\ln q_e = \ln K_f + \frac{1}{n}\ln C_e \quad (9)$$

Tempkin

$$q_e = K_t \cdot \ln(at) + K_t \cdot \ln C_e \quad (10)$$

D-R

$$\ln q_e = \ln q_m - \beta\varepsilon^2 \quad (11)$$

$$\varepsilon = RT\ln[1+(1/C_e)] \quad (12)$$

$$E = \frac{1}{\sqrt{2\beta}} \quad (13)$$

K_f, R_L, and Ks are the constants for the Langmuir, Freundlich and Tempkin models, respectively. C_e is the dye concentration after adsorption, q_e, and q_{max} are capacity of adsorption at time t, and maximum adsorption, respectively. n means strength of the adsorption process, and if it is between 1, and 10, it means that the adsorption process is favorable. R is the gas constant (8.314 J K^{-1}mol^{-1}), T is the absolute temperature in Kelvin, β indicates the mean free energy of sorption per molecule of sorbate.

Results and Discussion

Characterization of Polymer Particles

FT-IR analyses were perfomed to evaluate that the synthesis and modifications of PGMA gels were successful. FT-IR spectra of PGMA, and PGMA-EDA are given in Figure 3. When Figure 3A was examined for PGMA; it was determined that the peaks observed at 3000 and 2934 cm^{-1} were the stretching belonging to aliphatic C-H bonds in the polymer structure, the peak at 1721 cm^{-1} was the stretching belonging to the C=O group of the ester structure, the peak at 1250 cm^{-1} was the stretching belonging to both the C-O-C groups in the ester structure, and the C-O-C groups in the epoxy ring, the peak at 1133 cm^{-1} was the bending of the C-O-C group of the ester , and the peaks at 905, 842, and 754 cm^{-1} were typical stretching, and bending peaks belonging to the C-O-C groups in the epoxy ring.

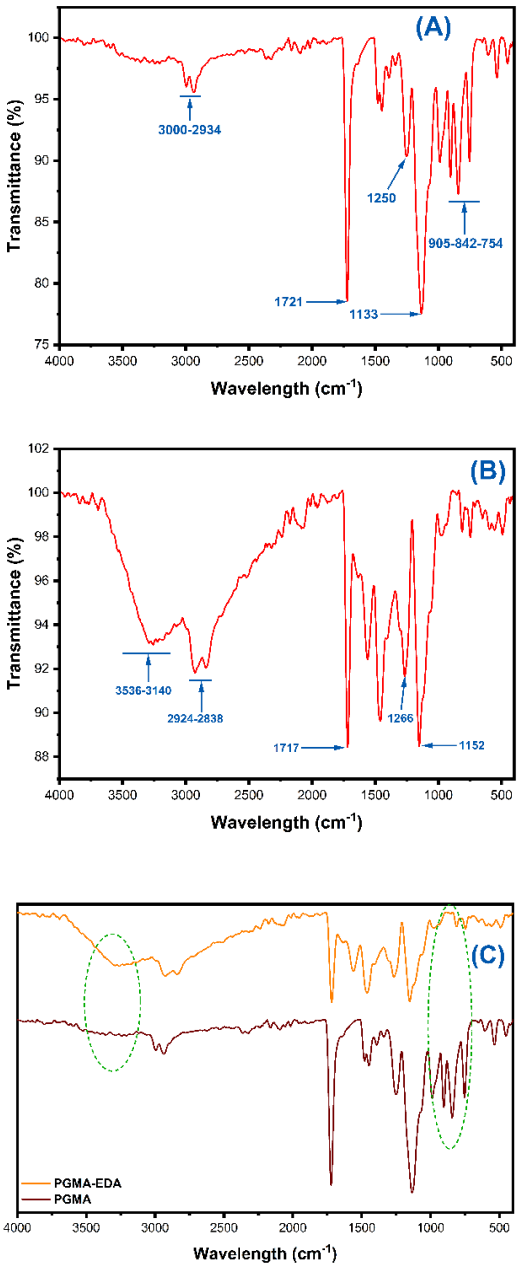

Figure 3. FT-IR spectra. PGMA (A), PGMA-EDA (B), and merged graphs (C).

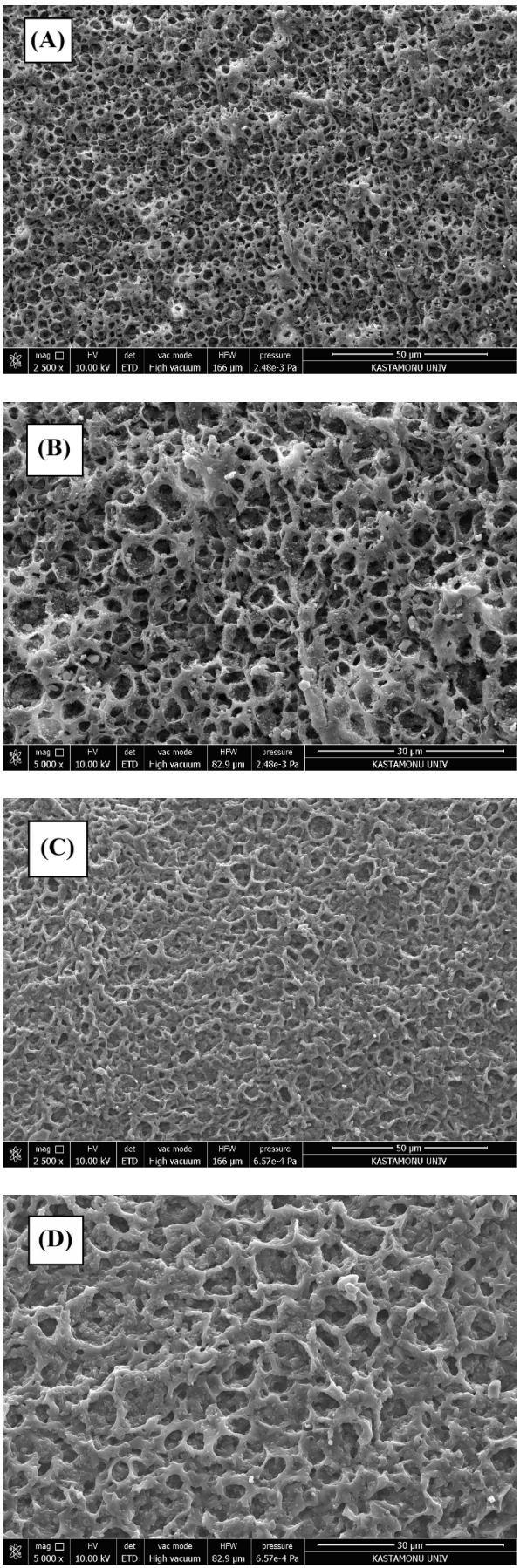

Figure 4. SEM images of PGMA (A) from 50 µm, (B) from 30 µm, and SEM images of PGMA-EDA (C) from 50 µm, (D) from 30 µm.

In PGMA-EDA gels, unlike PGMA, new peaks belonging to N-H, and NH_2 groups formed as a result of the reaction, and new peaks belonging to -OH group formed by the opening of the epoxy ring should be seen in the FT-IR spectrum. At the same time, the peaks belonging to this ring should disappear due to the opening of the epoxy ring. When the graph belonging to PGMA-EDA is examined in Figure 3, it was seen that the typical stretching vibrations belonging to N-H, and NH_2 groups were in the range of 3536-3140 cm^{-1}, and the peaks belonging to -OH group are widely located from 3700 to 2500 cm^{-1}. At the same time, it was understood that the peaks at 905, 842, and 754 cm^{-1} belonging to the epoxy ring of PGMA were not seen in the structure. These results were revealed that the PGMA gels were successfully modified.

The surface morphologies of PGMA gel, and PGMA-EDA were determined by SEM. The images obtained are presented in Figure 4. As it is known, polymeric gels have a weblike structure depending on the type, and size of the crosslinker used. Weblike structures in SEM images showed that polymeric gels were successfully obtained from GMA monomer (Figure 4A). However, this weblike structure was somewhat closed or filled after the modification of PGMA gels with EDA (Figure 4B). The main reason for this was the addition of a bulky molecule (EDA) to the structure of the polymer. This addition naturally led to a closure of the pores. However, the welike structure still remained as it is.

The thermal stabilities of the synthesized PGMA gels, and their modified forms (PGMA-EDA) within the scope of the study were revealed by TGA analyses. The obtained graphics are presented in Figure 5. Accordingly, the first mass loss for PGMA was observed at 133 °C. The mass loss at this temperature was 2.32%. The next mass loss started at 265 °C, and after this temperature, PGMA rapidly underwent thermal degradation. The mass loss was 3.03% up to 265 °C. This mass loss showed that the PGMA gel had a quite stable structure up to 265 °C. On the other h and the situation was slightly different in PGMA-EDA gels. The first mass losses started to be seen immediately after the polymer was heated and ended at 148 °C. It was calculated that PGMA-EDA lost 14.03% mass during this time. From 148 °C to 217 °C, the mass loss (4.17%) was not too much. However, immediately after this temperature, PGMA-EDA rapidly lost mass and degraded. The main reason for these rapid mass losses observed in PGMA-EDA ws thought to be due to the difference in hydrophilicity between PGMA and PGMA-EDA because PGMA is hydrophobic and does not retain water. However, after being modified with EDA, it has N-H, and O-H groups that can make strong hydrogen bonds. It was thought that these mass losses may be due to the removal of water in the structures of PGMA-EDA after washing. However, from the second mass loss, it was seen that the modification by amine groups seriously reduces the thermal stability of PGMA gels.

Adsorption Studies

Determination of contact time

Adsorption is a process in which the interactions between the adsorbent and adsorbate are balanced. Properly finding the contact time between the adsorbate and adsorbent is crucial for maximizing the efficiency of

the adsorbent. Insufficient contact time can hinder the effectiveness of the adsorption process. Otherwise, time and energy will be lost. For this reason, the equilibrium times for BPB were first determined in this study. The experiments were carried out for BPB between 5-360 minutes (100 mg L^{-1} BPB concentration, 25 ºC, and 30 mg PGMA-EDA gels, pH 4.3, and 300 rpm shaking speed) (Figure 6). According to the Figure 6, BPB was rapidly adsorbed onto PGMA-EDA gels (38.11 mg g^{-1}) until the 240th minute. After this, the adsorption increase stopped and did not change. For this reason, the adsorption equilibrium time for BPB was assumed to be 240 min.

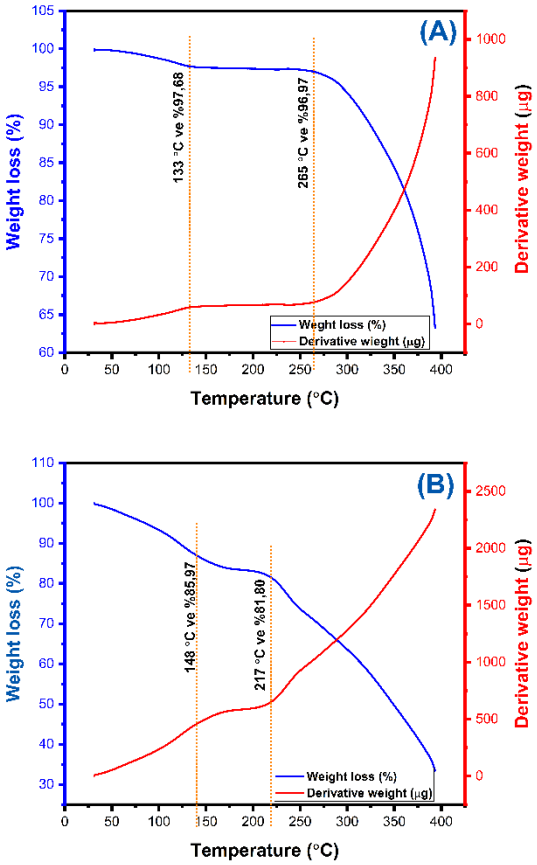

Figure 5. Thermogravimetric analyses of PGMA (A), and PGMA-EDA (B).

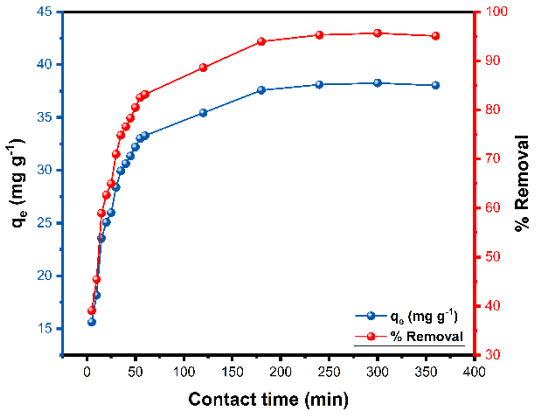

Figure 6. Adsorption equilibrium time graph obtained for PGMA-EDA gels.

Adsorption Kinetics

The adsorption rate is a critical factor to reveal the mechanism of the adsorption when selecting an effective adsorbent (Repo et al., 2011). Therefore, the mechanism between PGMA-EDA gels, and BPB were investigated via various kinetic models (PFO, PSO, ID, and the Elovich). The calculated results for the kinetic models were summarized in Table 1 and graphs were presented in Figure 7, respectively. The data obtained from contact time experiments were used to calculate the kinetic models.

The PFO model suggests that the occupancy adsorption rate sites are proportional to the occupied areas, while the PSO model argues that this ratio is related to the square of the occupied areas (Chien, 1963, Altaher et al., 2014). When PFO, and PSO correlation coefficients for BPB (0.734, and 0.999, respectively) were compared, it was seen that the PSO model had a higher R^2 value (0.999) (Figure 7A and B, respectively). When the q_e values for both models (17.71, and 39.53 mg g^{-1}, respectively) were compared with the experimental q_{exp} values (38.12 mg g^{-1}), it was seen that the values obtained with PSO were quite close to each other. These two situations showed that the BPB adsorption was more suitable for the PSO kinetic model. It appears that the rate-determining step could involve chemisorption, characterized by valence forces through electron sharing or exchange between PGMA-EDA gels and BPB molecules (Oter et al., 2024). Similar results were obtained in the literature (El-Zahhar et al., 2014; Gokkus et al., 2023; Gokkus et al., 2024; Oter et al., 2024)

The adsorption process typically occurs in three distinct stages over time. Firstly, dye molecules are transported from the liquid phase to the adsorbent surface through external diffusion. Secondly, the dye molecules diffuse internally into the pores of the adsorbent. Thirdly, chemical and/or physical bonds are formed between the active sites and the adsorbate within the adsorbent pores (Ahmed & Abou-Gamra, 2016). The non-linearity observed in the kinetic studies' graphs indicates that the adsorption process involves sequential steps and displays multiple linear phases. When the adsorption between PGMA-EDA gels, and BPB was evaluated using the ID model, the adsorption occured in two stages (Figure 7). In the first stage, the adsorption capacity rapidly reached 33.27 mg g^{-1}, and this rate decreased in the second stage. At the beginning of the process (first stage), since the surface-active sites of PGMA-EDA gels were empty, BPB molecules quickly adsorbed on these sites. Therefore, adsorption occurred rapidly in the first stage. In the second stage, it was observed that BPB molecules diffused into the macropores of PGMA-EDA gels, which decreased the adsorption rate.

Determination of adsorbent amount

Determination of the optimum adsorbent amount is extremely critical in order to prevent an increase in cost without a decrease in adsorption efficiency. If the amount of adsorbent is low, sufficient efficiency cannot be obtained from the adsorbent due to insufficient active site. Otherwise, adsorption will not be economical due to the use of excess adsorbent. For this reason, experiments were conducted to find the optimal amount of adsorbent (5, 15, 25, 35, and 50 mg). During the experiments, 25 ºC, 100 mg L^{-1} BPB concentration, pH 4.3, 10 mL volume, 300 rpm shaking speed, and 240 minutes were kept constant. The

maximum capacity of adsorption was determined as 5 mg adsorbent amount (68.74 mg g^{-1}), and the minimum capacity of adsorption was found as 50 mg adsorbent amount (19.33 mg g^{-1}) (Figure 8). When the results were evaluated, it was seen that the q_e decreased depending on the increase in the adsorbent amount. The adsorption capacity increased rapidly up to 25 mg PGMA-EDA amount (38.12 mg g-1 and 95.03%) and then the increase rate decreased obviously. Therefore, it was decided that the optimum amount of PGMA-EDA was 25 mg. The subsequent experiments were continued with 25 mg of PGMA-EDA. The most probable reason for this situation was thought to be the agglomeration of PGMA-EDA due to the low solution volume (10 mL). The aggregation of the gels prevented the distribution of BPB molecules on the adsorbent surface, and this effect became more pronounced when 50 mg of adsorbent was used. Alver & Metin (2012) reported in their studies that the adsorbent amount positively affected the adsorption process up to a certain extent, and then the efficiency decreased because of the agglomeration of the adsorbent. Bulut & Aydın (2006) reported similar results, and implied that this was due to some regions not reaching full saturation during adsorption. These results were also obtained in the other studies (Jirekar et al., 2014; Lapwanit et al., 2018).

Table 1. BPB adsorption kinetic parameters on PGMA-EDA gels.

Kinetic models	Parameters	BPB
PFO	q_e (mg.g^{-1})	38.12
	k_1 (min^{-1})	0.003
	R^2	0.734
	q_{exp} (mg.g^{-1})	17.71
PSO	q_e (mg.g^{-1})	38.12
	k_2 (g.mg^{-1}.min^{-1})	2.28×10^{-3}
	R^2	0.999
	q_{exp} (mg.g^{-1})	39.53
ID	k_i (mg. g^{-1}min$^{-1/2}$)	0.867
	I (mg.g^{-1})	20.66
	R^2	0.737
Elovich	α (mg.g^{-1}min^{-1})	0.183
	β (g.mg^{-1})	27.91
	R^2	0.93

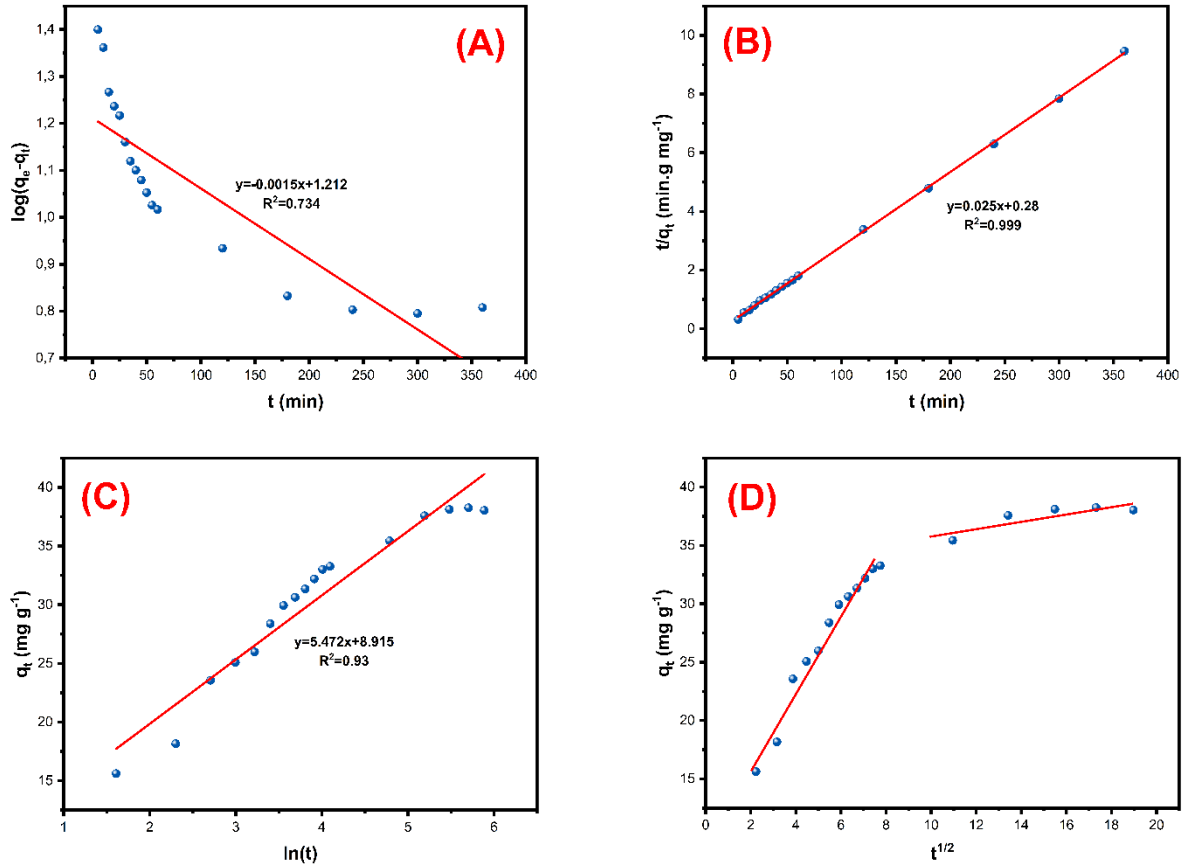

Figure 7. PFO (A), PSO (B), Elovich (C), and ID (D) kinetic models for the adsorption of BPB onto PGMA-EDA.

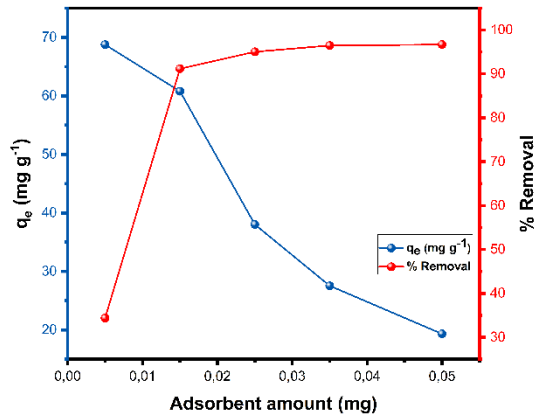

Figure 8. Effect of PGMA-EDA gel amounts on the adsorption of BPB dye.

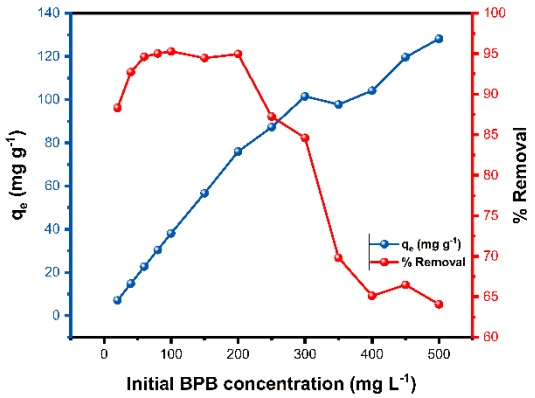

Figure 9. Effect of initial BPB dye concentration on adsorption.

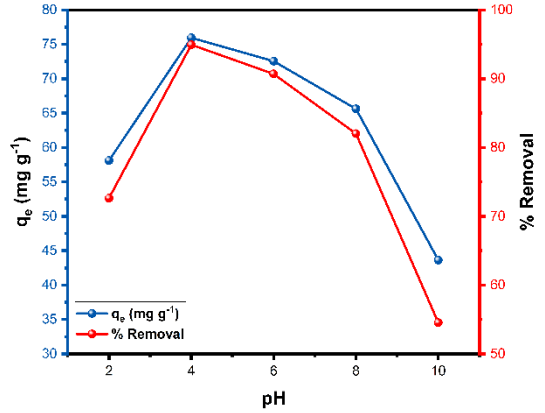

Figure 10. Effect of pH.

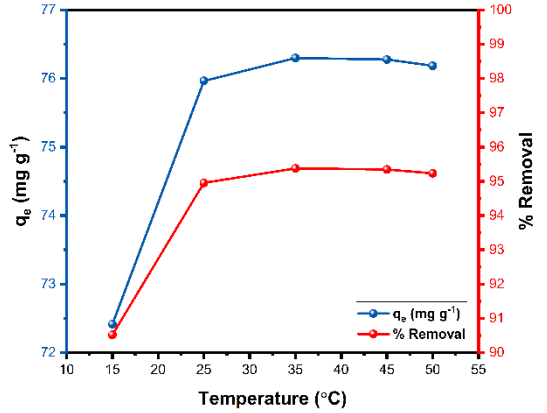

Figure 11. Effect of temperature on the adsorption of BPB.

Determination of initial dye concentration

To evaluate potential or capacity of an adsorbent, determination of the optimum dye concentration is an important parameter. Therefore, the optimum BPB concentration was determined for PGMA-EDA gels with 20 - 500 mg L^{-1} of concentrations (Figure 9). During the experiments, 25 ºC, 25 mg PGMA-EDA gels, pH 4.3, 10 mL solution volume, 300 rpm shaking speed were kept constant. The findings are presented in Figure 9. The adsorption capacities of PGMA-EDA gels showed a continuous increase from 20 mg L^{-1} to 500 mg L^{-1} BPB concentration. Meanwhile, the adsorption capacity raised from 7.06 mg g^{-1} to 128.15 mg g^{-1}. The highest q_e value was obtained with 128.15 mg g^{-1} for 500 mg L^{-1} BPB concentration. However, at this concentration, % removal efficiency decreased below 65%. At 200 mg L^{-1} BPB concentration, q_e value was 75.96 mg g^{-1} corresponding to removal efficiency of 94.96%, and at 250 mg L^{-1} concentration, q_e was calculated 87.24 mg g^{-1} corresponding to removal efficiency of 87.24%. Since the efficiency decreased below 90% at 250 mg L^{-1} concentration, it was decided that the optimum BPB concentration for PGMA-EDA gels was 200 mg L^{-1}. Subsequent experiments were continued with this concentration. The increasing of the adsorption capacity (q_e) with the increasing BPB concentration could be revealed by the repulsion of the BPB molecules. With the effect of these repulsion forces, BPB quickly adhered to the surface of PGMA-EDA gels. This repulsion also increased the adsorption rate and diffusion of BPB into the pores of PGMA-EDA gels. To increase the concentration also caused a raised in the amount of dye adsorbed. This observation was consistent with literature (Gürses et al., 2006; Yagub et al., 2014). If the dye concentration was increased, the available adsorption sites' number decreased and therefore the effect of BPB removal varied depending on the initial BPB concentration and the dyes were physically adsorbed only to the adsorbent's outer surface with a single layer (Mahmoodi et al., 2011).

Effect of pH

pH significantly affects the adsorption process by changing the protonation degree and surface charge of functional groups on adsorbents and dyes. Therefore, determining the optimum pH for adsorption is of critical importance. Therefore, in this study, adsorption of BPB dye by PGMA-EDA gels was carried out with 2, 4, 6, 8, and 10 pHs at 25 ºC, 25 mg PGMA-EDA gels, 200 mg L^{-1} BPB concentration, 10 mL sample volume, 300 rpm shaking speed. The minimum adsorption of BPB was determined at pH 10 (43.64 mg g^{-1}), and the highest adsorption was obtained at pH 4 (75.96 mg g^{-1}) (Figure 10). PGMA-EDA contains abundant amine groups in its structure. Since these groups are protonated in acidic environments, the surface charges of PGMA-EDA gels increase. In contrast, BPB dye is anionic. Therefore, PGMA-EDA being more cationic at pH 4 led to an increase in the electrostatic attraction force between it and BPB. Thus, the adsorption capacity of PGMA-EDA was the

highest at pH 4. The number of protons increased considerably at pH 2. It is thought that this caused the protons to adsorb on the surface of BPB. Therefore, the adsorption efficiency of PGMA-EDA decreased at pH 2. Similar results were reported in other studies (Liu et al., 2014; Dhananasekaran et al., 2016; Gokkus et al., 2024).

Adsorption thermodynamics and effect of temperature

The experiments were conducted at varying temperatures (15–50 °C) keeping the conditions of 25 mg PGMA-EDA gel, pH 4, 10 mL solution volume, 300 rpm shaking speed, 200 mg L^{-1} BPB concentration, and 240 minutes constant. Therefore, the effect of temperature on the adsorption process was evaluated. The lowest adsorption capacity was observed as 72.41 mg g^{-1} at 15 °C, while the highest was recorded as 76.3 mg g^{-1} at 30 °C. The findings indicated a slight increase in the capacity of adsorption when the temperature rose from 25 °C to 50 °C (Figure 11). The increasing of adsorption efficiency with the increasing of temperature was revealed the process was endothermic. This meant that higher temperatures facilitate greater adsorption of BPB molecules onto the PGMA-EDA gel (Figure 11). Similar trends were obtained by Al-Ghouti et al. (2005) and Gürses et al. (2006).

Thermodynamic evaluation of adsorption processes is of great importance in terms of determining whether these processes are spontaneous or not (Sun & Wang, 2010). Therefore, Gibbs free energy (ΔG°), enthalpy (ΔH°), and entropy (ΔS°) changes were calculated from the temperature reults. According to the data in Table 2, ΔG° was calculated as 4.19 kJ mol^{-1}. A positive ΔG° value indicates that the adsorption of BPB occurred spontaneously. ΔH° represents the enthalpy change during the reaction; a negative value signifies an exothermic reaction, while a positive value indicates an endothermic reaction. As the calculated ΔH° value was determined to be 14.39 kJ mol^{-1}, it was concluded that the adsorption between PGMA-EDA gels, and BPB was endothermic. A negative ΔS° value indicates that the randomness decreased during adsorption and the reaction became less disordered. According to the experimental results, the ΔS° value for PGMA-EDA gels was found to be -64.46 J mol^{-1}. This highlighted the decreasing irregularity of the adsorption process between PGMA-EDA gels and BPB. The optimum adsorption conditions of PGMA-EDA on the adsorption of BPB dye were summarized in the Table 3.

Table 2. Thermodynamic parameters of BPB adsorption on PGMA-EDA gels.

Temperature (°C)	ΔH°(kJ mol^{-1})	ΔS°(J $mol^{-1}K^{-1}$)	TΔS°(kJ mol^{-1})	ΔG°(kJ mol^{-1})
15				
25				
35	14.39	-64.46	-18.58	4.19
45				
50				

Table 3. Optimum conditions obtained for the adsorption of BPB dye for PGMA-EDA gels.

Parameters	BPB
pH	4
Temperature (ºC)	25
Initial BPB conc. (mg L^{-1})	200
PGMA-EDA amount (mg)	25
Equilibrium time (min)	240

Table 4. Isotherm parameters of BPB adsorption on PGMA-EDA gels

Isotherms	Parameters	BPB
Langmuir	q_{max} (mg.g^{-1})	128.15
	$q_{e,exp}$ (mg.g^{-1})	125.0
	K_L (L.mg^{-1})	0.057
	R_L	0.23
	R^2	0.97
Freundlich	K_f[(mg.g^{-1})(L.mg^{-1})$^{1/n}$)]	12.88
	n	2.11
	R^2	0.77
Temkin	β_T	24.19
	KT (L.g^{-1})	1.04
	R^2	0.94
Dubinin-Radushkevich	q_{max} (mg·g^{-1})	128.15
	$q_{e,exp}$ (mg.g^{-1})	98.4
	β (mol^{-2}.J^{-2})	3.49
	E (kJ.mol^{-1})	0.38
	R^2	0.97

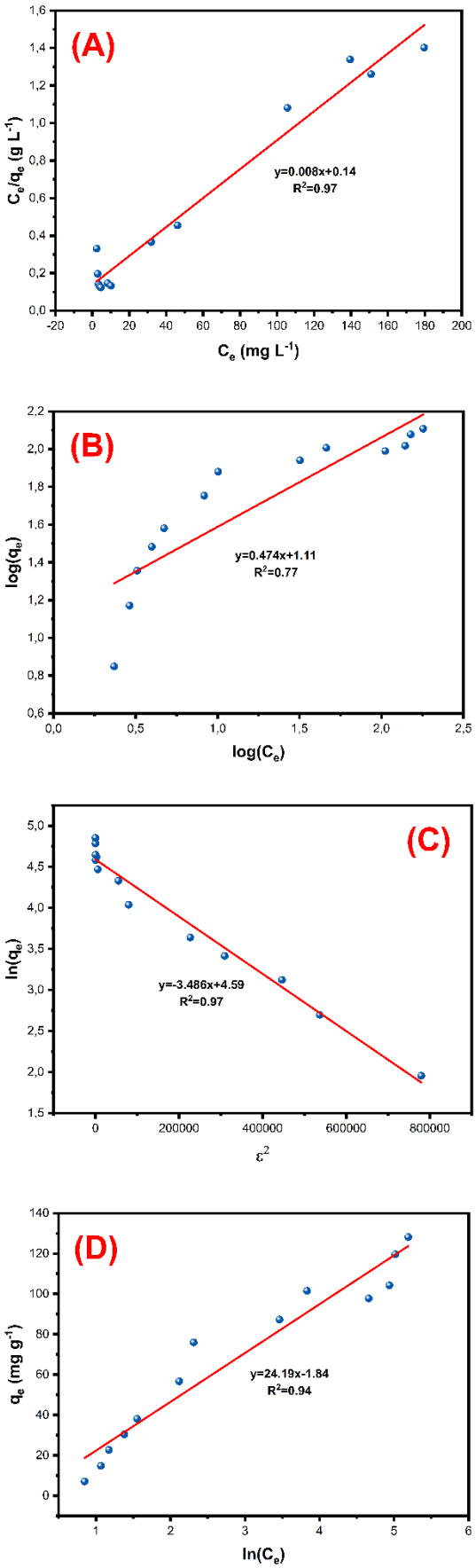

Figure 12. Langmuir (A), Freundlich (B) Dubinnin-Radushkevic (C), and Temkin (D) isotherms of BPB on the synthesized PGMA-EDA gels.

Adsorption isotherms

The adsorption between BPB and PGMA-EDA gels was analyzed using experimental data based on the Freundlich, Langmuir, Dubinin-Radushkevich (DR), and Temkin isotherm models. The isotherm parameters for BPB adsorption on PGMA-EDA gels are summarized in Table 4, while the corresponding isotherm graphs are presented in Figure 12. Among the models, Langmuir isotherm value (the highest; 0.97), indicating that the adsorption occurs on a monolayer and homogeneous surface. This conclusion was further supported by the calculated (q_m; 128.15 mg g^{-1}), and experimental (q_e; 125.0 mg g^{-1}) values. Additionally, the correlation values for the Temkin, and D-R isotherms were calculated as 0.94, and 0.97, respectively, as shown in Table 4, highlighting the compatibility of these models with the adsorption process on PGMA-EDA gels. In a similar study, the removal capacity of poly(quaternary ammonium salt) in the removal of Acid Red 18 (AR18) , and Acid Blue 25 (AB25) dyes was investigated under both single, and binary systems. It was reported that Langmuir isotherm demonstrated the best fit to the equilibrium data, indicating maximum monolayer adsorption (Mahmoodi et al., 2011).

Conclusion

This study focused on the efficient removal of BPB dye, which is used intensively in the industry. For this purpose, PGMA gels were modified to produce PGMA-EDA gels and used in the adsorption of BPB dye. Adsorption was performed according to the 'batch adsorption' method in three replicates. In the study, the optimum pH, temperature, contact time, shaking speed, dye concentration, and adsorbent amount for PGMA-EDA gels were determined. pH 4, 25 °C, 240 mins, 200 mg L^{-1} BPB concentration, and 25 mg PGMA-EDA amount were determined the optimum adsorption conditions for PGMA-EDA gels.

In order to elucidate the adsorption mechanism, Langmuir, Freundlich, Temkin, and Dubinin-Radushkevich isotherms were performed with the data obtained from the initial dye concentration experiments. On the other hand, calculations of PFO, and PSO kinetic models were performed with the contact time data. As a result of these calculations, the highest R^2 value among the isotherm models for BPB was obtained for the Langmuir isotherm. This result showed that the adsorption occured in a monolayer and homogeneous structure and when the correlation coefficients calculated with PFO, and PSO models for BPB were compared, it was seen that the PSO model had a higher R^2 value. This showed that the BPB adsorption was more suitable for the PFO kinetic model.

Declarations

The authors declare that they have no known competing financial interests or personal relationships that could have appeared to influence the work reported in this paper.

References

Abubakar, S. I., & Ibrahim, M. B. (2018). Adsorption of bromophenol blue and bromothymol blue dyes onto raw maize cob. Bayero Journal of Pure and Applied Sciences, 11(1), 273-281. DOI: 10.4314/bajopas.v11i1.45S

Ahmed, M. A., & Abou-Gamra, Z. M. (2016). Mesoporous MgO nanoparticles as a potential sorbent for removal of fast orange and bromophenol blue dyes. Nanotechnology for Environmental Engineering, 1, 1-11. DOI: https://doi.org/10.1007/s41204-016-0010-7

Akpomie, K. G., Adegoke, K. A., Oyedotun, K. O., Ighalo, J. O., Amaku, J. F., Olisah, C., ... & Conradie, J. (2024). Removal of bromophenol blue dye from water onto biomass, activated carbon, biochar, polymer, nanoparticle, and composite adsorbents. Biomass Conversion and Biorefinery, 14(13), 13629-13657. DOI: https://doi.org/10.1007/s13399-022-03592-w

Al-Ghouti, M., Khraisheh, M. A. M., Ahmad, M. N. M., & Allen, S. (2005). Thermodynamic behaviour and the effect of temperature on the removal of dyes from aqueous solution using modified diatomite: a kinetic study. Journal of Colloid and Interface Science, 287(1), 6-13. DOI: https://doi.org/10.1016/j.jcis.2005.02.002

Altaher, H., Khalil, T. E., & Abubeah, R. (2014). The effect of dye chemical structure on adsorption on activated carbon: a comparative study. Coloration Technology, 130(3), 205-214. DOI: https://doi.org/10.1111/cote.12086

Alver, E., & Metin, A. Ü. (2012). Anionic dye removal from aqueous solutions using modified zeolite: Adsorption kinetics and isotherm studies. Chemical Engineering Journal, 200, 59-67. DOI: https://doi.org/10.1016/j.cej.2012.06.038

Benjelloun, M., Miyah, Y., Evrendilek, G. A., Zerrouq, F., & Lairini, S. (2021). Recent advances in adsorption kinetic models: their application to dye types. Arabian Journal of Chemistry, 14(4), 103031. DOI: https://doi.org/10.1016/j.arabjc.2021.103031

Bulut, Y., & Aydın, H. (2006). A kinetics and thermodynamics study of methylene blue adsorption on wheat shells. Desalination, 194(1-3), 259-267. DOI: https://doi.org/10.1016/j.desal.2005.10.032

Chien, J. C. (1963). Kinetics of propylene polymerization catalyzed by α-titanium trichloride–diethylaluminum chloride. Journal of Polymer Science Part A: General Papers, 1(1), 425-442. DOI: https://doi.org/10.1002/pol.1963.100010138

Chien, S., and W. Clayton. (1980). Application of Elovich equation to the kinetics of phosphate release and sorption in soils. Soil Science Society of America Journal. DOI: https://doi.org/10.2136/sssaj1980.03615995004400020013x

Dhananasekaran, S., Palanivel, R., & Pappu, S. (2016). Adsorption of methylene blue, bromophenol blue, and coomassie brilliant blue by α-chitin nanoparticles. Journal of advanced research, 7(1), 113-124. DOI: https://doi.org/10.1016/j.jare.2015.03.003

El-Zahhar, A. A., Awwad, N. S., & El-Katori, E. E. (2014). Removal of bromophenol blue dye from industrial waste water by synthesizing polymer-clay composite. Journal of molecular liquids, 199, 454-461. DOI: https://doi.org/10.1016/j.molliq.2014.07.034

Freundlich, H.M.F. (1906). Over the adsorption in solution. J. Phys. chem, 57(385471): p. 1100-1107.

Ghaedi, M., Ghayedi, M., Kokhdan, S. N., Sahraei, R., & Daneshfar, A. (2013). Palladium, silver, , and zinc oxide nanoparticles loaded on activated carbon as adsorbent for removal of bromophenol red from aqueous solution. Journal of Industrial and Engineering Chemistry, 19(4), 1209-1217. DOI: https://doi.org/10.1016/j.jiec.2012.12.020

Gokkus, K., Sengel, S. B., Yildirim, Y., Hasanbeyoglu, S., & Butun, V. (2023). Amine-functionalised poly (glycidyl methacrylate) hydrogels for Congo red adsorption. Journal of Environmental Engineering and Science, 18(4), 204-214. DOI: https://doi.org/10.1680/jenes.23.00025

Gokkus, K., Oter, C., Amlani, M., Gur, M., & Butun, V. (2024). Preparation of versatile polymer particles and their application for elimination of bromophenol blue and phenol from aqueous environment. Desalination and Water Treatment, 318, 100402. DOI: https://doi.org/10.1016/j.dwt.2024.100402

Gürses, A., Doğar, Ç., Yalcın, M., Açıkyıldız, M., Bayrak, R., & Karaca, S. (2006). The adsorption kinetics of the cationic dye, methylene blue, onto clay. Journal of Hazardous Materials, 131(1-3), 217-228. DOI: https://doi.org/10.1016/j.jhazmat.2005.09.036

Ho, Y.-S., and G. McKay (1999). Pseudo-second order model for sorption processes. Process biochemistry.

Jirekar, D. B., Pathan, A. A., & Farooqui, M. (2014). Adsorption studies of methylene blue dye from aqueous solution onto Phaseolus aureus biomaterials. Orient J Chem, 30(3), 1263-1269. DOI: http://dx.doi.org/10.13005/ojc/300342

Katheresan, V., Kansedo, J., & Lau, S. Y. (2018). Efficiency of various recent wastewater dye removal methods: A review. Journal of environmental chemical engineering, 6(4), 4676-4697. DOI: https://doi.org/10.1016/j.jece.2018.06.060

Lagergren, S. (1898). About the theory of so-called adsorption of soluble substances.

Langmuir, I. (1916). The constitution and fundamental properties of solids and liquids. Part I. Solids. Journal of the American chemical society, 38(11): p. 2221-2295.

Lapwanit, S., Sooksimuang, T., & Trakulsujaritchok, T. (2018). Adsorptive removal of cationic methylene blue dye by kappa-carrageenan/poly (glycidyl methacrylate) hydrogel beads: preparation and characterization. Journal of environmental chemical engineering, 6(5), 6221-6230. DOI: https://doi.org/10.1016/j.jece.2018.09.050

Liu, J., Yao, S., Wang, L., Zhu, W., Xu, J., & Song, H. (2014). Adsorption of bromophenol blue from aqueous samples by novel supported ionic liquids. Journal of Chemical Technology & Biotechnology, 89(2), 230-238. DOI: https://doi.org/10.1002/jctb.4106

Mahmoodi, N. M., Salehi, R., Arami, M., & Bahrami, H. (2011). Dye removal from colored textile wastewater using chitosan in binary systems. Desalination, 267(1), 64-72. DOI: https://doi.org/10.1016/j.desal.2010.09.007

Malik, P. K. (2004). Dye removal from wastewater using activated carbon developed from sawdust: adsorption equilibrium and kinetics. Journal of Hazardous Materials, 113(1-3), 81-88. DOI: https://doi.org/10.1016/j.jhazmat.2004.05.022

Mashkoor, F., & Nasar, A. (2020). Magsorbents: Potential c, andidates in wastewater treatment technology–A review on the removal of methylene blue dye. Journal of magnetism and magnetic materials, 500, 166408. DOI: https://doi.org/10.1016/j.jmmm.2020.166408

Mezohegyi, G., van der Zee, F. P., Font, J., Fortuny, A., & Fabregat, A. (2012). Towards advanced aqueous dye removal processes: a short review on the versatile role of activated carbon. Journal of environmental management, 102, 148-164. DOI: https://doi.org/10.1016/j.jenvman.2012.02.021

Mokif, L. A. (2019). Removal methods of synthetic dyes from industrial wastewater: a review. Mesopotamia Environmental Journal (mesop. environ. j) ISSN: 2410-2598, 5(1), 23-40. DOI: http://dx.doi.org/10.31759/mej.2019.5.1.0040

Moradihamedani, P. (2022). Recent advances in dye removal from wastewater by membrane technology: a review. Polymer Bulletin, 79(4), 2603-2631. DOI: https://doi.org/10.1007/s00289-021-03603-2

Morais, L. C., Freitas, O. M., Goncalves, E. P., Vasconcelos, L. T., & Beca, C. G. (1999). Reactive dyes removal from wastewaters by adsorption on eucalyptus bark: variables that define the process. Water Research, 33(4), 979-988. DOI: https://doi.org/10.1016/S0043-1354(98)00294-2

Namasivayam, C., Jeyakumar, R., & Yamuna, R. T. (1994). Dye removal from wastewater by adsorption on 'waste'Fe (III)/Cr (III) hydroxide. Waste management, 14(7), 643-648. DOI: https://doi.org/10.1016/0956-053X(94)90036-1

Navin, P. K., Kumar, S., & Mathur, M. (2018). Textile wastewater treatment: a critical review. Int J Eng Res Technol, 6(11), 1-7.

Oter, C., Gokkus, K., Gur, M., & Butun, V. (2024). Polymeric Adsorbent for the Effective Removal of Toxic Dyes from Aqueous Solutions: Equilibrium, Kinetic, and Thermodynamic Modeling. ChemistrySelect, 9(42), e202403526. DOI: https://doi.org/10.1002/slct.202403526

Radushkevich, M. (1947). The equation of the characteristic curve of the activated charcoal USSR Phys. Chem Sect, 55: p. 331.

Raman, C. D., & Kanmani, S. J. J. E. M. (2016). Textile dye degradation using nano zero valent iron: a review. Journal of Environmental Management, 177, 341-355. DOI: https://doi.org/10.1016/j.jenvman.2016.04.034

Repo, E., Warchoł, J. K., Bhatnagar, A., & Sillanpää, M. (2011). Heavy metals adsorption by novel EDTA-modified chitosan–silica hybrid materials. Journal of colloid and interface science, 358(1), 261-267. DOI: https://doi.org/10.1016/j.jcis.2011.02.059

Sun, C. L., & Wang, C. S. (2010). Estimation on the intramolecular hydrogen-bonding energies in proteins and peptides by the analytic potential energy function. Journal of Molecular Structure: THEOCHEM, 956(1-3), 38-43. DOI: https://doi.org/10.1016/j.theochem.2010.06.020

Tempkin, M., and V. Pyzhev. (1940). Kinetics of ammonia synthesis on promoted iron catalyst. Acta Phys. Chim. USSR, 12(1): p. 327.

Weber Jr, W.J., and J.C. Morris. (1963). Kinetics of adsorption on carbon from solution. Journal of the sanitary engineering division.

Yagub, M. T., Sen, T. K., Afroze, S., & Ang, H. M. (2014). Dye and its removal from aqueous solution by adsorption: a review. Advances in colloid and interface science, 209, 172-184. DOI: https://doi.org/10.1016/j.cis.2014.04.002

Yao, X., Ji, L., Guo, J., Ge, S., Lu, W., Chen, Y., Song, W. (2020). An Abundant Porous Biochar Material Derived from Wakame (Undaria Pinnatifida) with High Adsorption Performance for Three Organic Dyes. Bioresource Technology, 318, 124082. DOI: https://doi.org/10.1016/j.biortech.2020.124082